

Multi-scale modeling and advanced simulation of concentrated fibrous suspensions

Francisco Chinesta¹, Emmanuelle Abisset-Chavanne¹ and Roland Keunings²

¹ GeM Institute, Ecole Centrale de Nantes, Nantes, France

² ICTEAM, Université catholique de Louvain, Louvain, Belgium

ABSTRACT

Most theoretical fiber suspension models currently used for predicting the flow-induced evolution of microstructure in the processing of reinforced thermoplastics are based on the Jeffery model for dilute suspensions or phenomenological adaptations of it. In most industrial applications, the concentration of fibers is usually large, so that intense fiber-fiber interactions occur that can affect their kinematics as well as activate bending. Moreover, complex microstructures are observed, as fibers aggregate in clusters with specific kinematics and deformability. At sufficiently high concentration, the suspension becomes fully entangled. Other processes involve fibers that are long compared to the typical flow dimensions, in which case classical first-gradient theories become inadequate for describing the fiber kinematics. Finally, many questions remain open, e.g. confinement and wall effects in the case of processes involving narrow gaps, and non-Newtonian suspending fluids. In this work, we revisit standard models and discuss their validity and limitations. We also point to our recent work on the modelling of fiber aggregates.

INTRODUCTION

Fiber suspensions can be described at different scales: (i) the microscopic scale, related to individual fibers, (ii) the

mesoscopic scale, which considers a population of fibers within a local representative volume, and (iii) the macroscopic scale related to the forming process and the final part itself.

Theoretical models not only depend on the chosen scale of description, but also on the concentration regime considered. In the dilute regime, fiber-fiber interactions are neglected altogether. These interactions are usually taken into account in the form of a phenomenological randomizing mechanism when the suspension is semi-dilute. In the semi-concentrated and concentrated regimes, such a phenomenological approach is no longer appropriate. Indeed, when the concentration and fiber length become large enough, richer microstructures can be observed: (i) entangled systems exhibiting numerous and intense interactions, and (ii) dense (either rigid or deformable) clusters of fibers immersed in the suspending fluid, with specific kinematics and often complex aggregation/disaggregation kinetics.

It is well known that the process-induced microstructure determines the mechanical or functional properties of the final part. Thus, the development of accurate models and efficient computational solvers is crucial. Industrial applications usually involve semi-concentrated or concentrated short fiber suspensions, as well as composites elaborated from SMC and derived technologies. These applications are thus

characterized by high fiber content, strong interactions, confinement and fiber bending mechanisms. They call for theoretical models that go much beyond the dilute regime.

Most currently available process simulation tools implement *ad-hoc* modifications of the classical Jeffery model developed for the dilute regime. In this paper, we revisit the most usual theoretical descriptions at different scales and concentration regimes, pointing out their strengths and weaknesses. We also point to our recent work on the modelling of fiber aggregates.

DIFFERENT DESCRIPTION SCALES

Suspensions of particles can be described at the microscopic scale by tracking the motion of each individual particle in the system. In the dilute regime, the motion of ellipsoidal particles immersed in a Newtonian fluid is accurately described by Jeffery's equation¹. For ellipsoids of infinite aspect ratio (rods) the Jeffery's equation reads

$$\dot{\mathbf{p}} = \nabla \mathbf{v} \cdot \mathbf{p} - (\mathbf{p}^T \cdot \nabla \mathbf{v} \cdot \mathbf{p}) \mathbf{p} \quad (1)$$

where \mathbf{p} is the unit vector defining the rod orientation and \mathbf{v} the fluid velocity assumed unperturbed by the rods presence and orientation.

In order to circumvent the difficulties (more computational than conceptual) related to simulations at the microscopic scale where too many particles are present, coarser models were introduced. The recent book² gives an overview of multi-scale approaches in computational rheology of rod suspensions.

Mesoscopic kinetic theory models result from the coarsening of microscopic descriptions. In kinetic theory models, the individuality of the particles is lost in favour of a statistical description that substitutes the entities by a series of conformation

coordinates³. For example, when considering a suspension of rods, the mesoscopic description consists in giving the fraction of rods $\Psi(\mathbf{x}, t, \mathbf{p})$ that at position \mathbf{x} and time t are oriented along direction \mathbf{p} . This information is contained in the probability distribution function (pdf) whose conservation balance results in the so-called Fokker-Planck equation

$$\frac{\partial \Psi}{\partial t} + \mathbf{v} \cdot \nabla_{\mathbf{x}} \Psi + \nabla_{\mathbf{p}} \cdot (\dot{\mathbf{p}} \Psi) = 0 \quad (2)$$

The Fokker-Planck equation governs the flow-induced evolution of conformation. Being highly-dimensional, it cannot be solved by means of standard mesh-based discretization techniques. This issue is known as the curse of dimensionality. Solution procedures based on the use of particles at the mesoscopic scale have been extensively developed by many authors^{4,5}. On the other hand, there are few works on the solution of the Fokker-Planck equation with standard discretization techniques⁶.

We have proposed in⁷ a new solution technique called Proper Generalized Decomposition (PGD) that allows for the direct solution of the Fokker-Planck equation in conformation spaces of high dimension. The PGD is based on the use of separated representations in order to ensure that the complexity scales linearly with the model dimensionality. It consists in expressing the unknown field as a finite sum of functional products, i.e. one approximates a generic multidimensional function $u(x_1, \dots, x_d)$ as

$$u(x_1, \dots, x_d) \approx \sum_{i=1}^N F_i^1(x_1) \dots F_i^d(x_d) \quad (3)$$

For more information on the PGD and its applications in computational rheology, see the recent book⁸.

At the macroscopic scale, the pdf is substituted by some of its moments⁹. Thus, for example the second order tensor (the odd

moments vanish because the symmetry of the pdf) reads

$$\mathbf{a}(\mathbf{x}, t) = \oint \mathbf{p} \otimes \mathbf{p} \Psi(\mathbf{x}, t, \mathbf{p}) d\mathbf{p} \quad (4)$$

Here, the level of detail and the involved physics are sacrificed in favour of computational efficiency. The equations governing the time evolution of these moments usually involve closure approximations whose impact on the results can be important.

FROM DILUTE TO CONCENTRATED REGIMES

In the case of dilute suspensions of short fibers, the three scales have been extensively considered, and without major difficulties, to model the associated systems. Difficulties appear, however, as soon as the concentration increases. In the semi-dilute regime, fiber-fiber interactions occur, but in general they can be accurately modelled by introducing a randomizing diffusion term in Jeffery's model¹⁰.

There is a wide literature concerning dilute and semi-dilute suspensions, addressing modelling, flows and rheology¹¹. These models describe quite well the experimental observations.

When the concentration increases further, intense fiber-fiber interactions occur which must be taken into account appropriately. In¹² an anisotropic rotary diffusion is proposed that accounts for the fiber-fiber interactions; the model parameters were selected by matching the experimental steady-state orientation in simple shear flow and by requiring stable steady states and physically realizable solutions.

The most complex scenario is that of the concentrated flow regime involving entangled suspensions or dense clusters immersed into the suspending fluid, exhibiting specific kinematics and complex aggregation / disaggregation mechanisms¹³.

The first natural question is how to describe such systems.

At the macroscopic scale, one could try to fit some power-law constitutive equation, however, this description does not hold for the microstructure. At the microscopic scale, direct numerical simulations describing complex fiber-fiber interactions can be carried out in small enough representative volumes.

A first attempt to describe dilute suspensions composed of rigid and deformable clusters from a micromechanical point of view was proposed. Later, kinematic predictions for rigid and deformable clusters were compared with direct numerical simulation. Enriched descriptions of the kinematics of rigid clusters within a multi-scale framework were then addressed. All these models are revisited in².

Finally, entangled systems involving moderately long fibers are generally described by using some *ad-hoc* adaptations of the Folgar-Tucker model. This model, however, has its origins in the Jeffery equation whose validity is by construction restricted to the dilute regime. For this reason, the validity of these models must be confirmed from both the theoretical and experimental viewpoints. Moreover, when the fiber length and the number of interactions per fiber increase, bending mechanisms are activated. Some attempts at modelling rod bending exist, and most of them consider the rod composed of rigid segments connected by springs activated by bending¹⁴.

SUSPENSIONS INVOLVING SHORT FIBERS

Taking the time derivative of equation (4) and considering (1) as well as a quadratic closure relation for the fourth order orientation tensor it results

$$\dot{\mathbf{a}} = \nabla \mathbf{v} \cdot \mathbf{a} + \mathbf{a} \cdot (\nabla \mathbf{v})^T - 2(\mathbf{a} : \mathbf{D})\mathbf{a} \quad (5)$$

Following the rationale detailed in² the Cauchy's stress reads

$$\boldsymbol{\sigma} = -p\mathbf{I} + 2\eta\mathbf{D} + 2\eta N_p (\mathbf{a} : \mathbf{D})\mathbf{a} \quad (6)$$

The flow model results of combining Eqs. (5) and (6) with the mass and momentum conservation balances

$$\begin{cases} \nabla \cdot \boldsymbol{\sigma} = \mathbf{0} \\ \nabla \cdot \mathbf{v} = 0 \end{cases} \quad (7)$$

Now, the solution of Eqs. (5)-(7) with appropriate initial and boundary conditions allows calculating the flow kinematics and the microstructure evolution from \mathbf{v} and \mathbf{a} respectively.

In the case of free or moving boundaries, the first encountered in steady state extrusion processes and the last in injection processes, the flow model must be complemented with extra-equations for defining the fluid domain. In the case of the free-boundaries these relations come from the stress-free condition on the free boundary. In the case of moving boundaries there are different alternative descriptions based on domain tracking or capturing.

Tracking strategies consist of moving the nodes located on the fluid boundary at each time step, with the material velocity, in order to describe the new fluid domain. The main issue related to this simple strategy is the mesh deformation that the simple nodes updating produces. Thus, frequent remeshing is required for ensuring the solution accuracy, but the price to be paid is the inevitable numerical diffusion when projecting variables from old to new meshes. Meshless methods have been largely employed in order to circumvent the just referred issues. They can update the nodal positions from the material velocities and the discretization remains accurate enough despite the very irregular nodal

distribution, avoiding the necessity of remeshing.

Domain capturing strategies proceeds by using a fixed mesh defined in the whole domain (e.g. mould) and a fluid presence function $I(\mathbf{x}, t)$ that indicates the presence of the fluid at position \mathbf{x} at time t . This function is convected with the material velocity according to

$$\frac{\partial I}{\partial t} + \mathbf{v} \cdot \nabla I = 0 \quad (8)$$

and from its value higher than a threshold value the fluid domain $\Omega_f(t)$ in which the flow model (5)-(7) is solved, is extracted.

Fig. 1 depicts the evolution of $\Omega_f(t)$ of a complex 3D part.

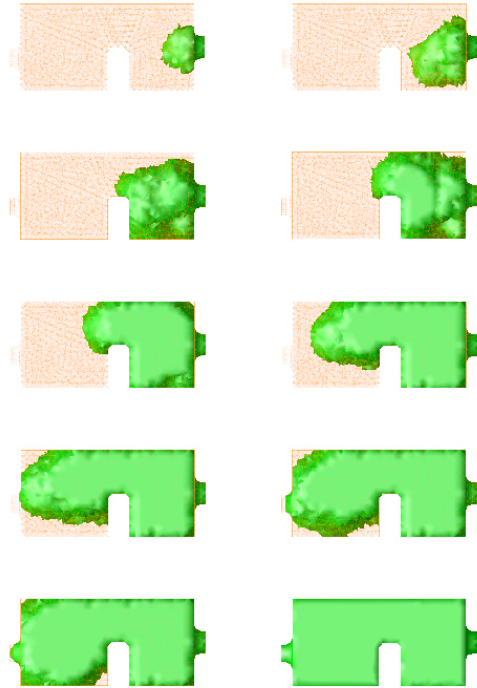


Figure 1. Fluid domain extracted from the presence of fluid function, during the injection process of a 3D part.

Fig. 2 shows the most probable fiber orientation that is quantified from the eigenvalues and eigenvectors of tensor \mathbf{a} . The eigenvector related to the higher eigenvalue is represented and the color indicates its magnitude. The red color indicates an orientation in the depicted direction whereas the blue color indicates a quasi-isotropic orientation (the three eigenvalues being 1/3)

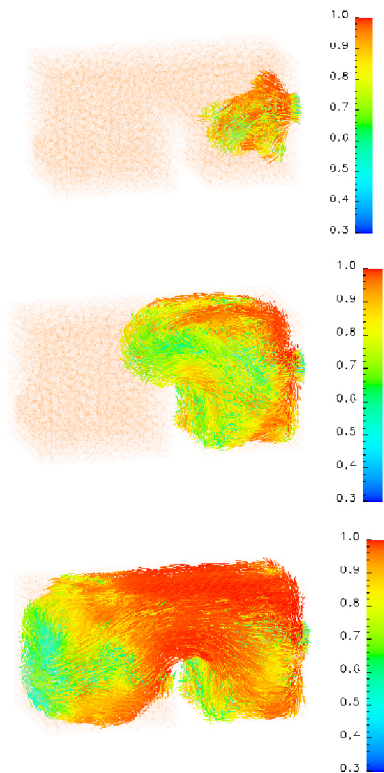


Figure 2. Fiber orientation state at three different steps of the filling process

A more complex scenario is considered in Figs. 3 and 4.

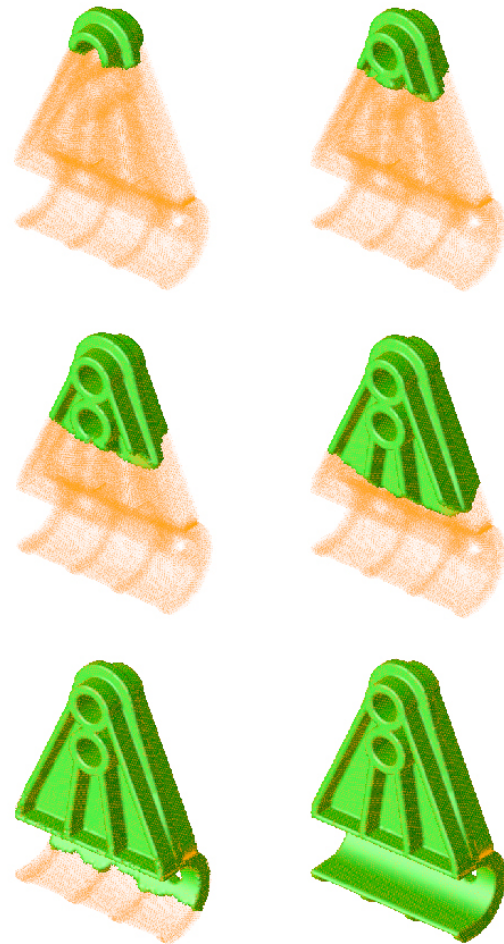


Figure 3. Fluid domain extracted from the presence of fluid function, during the injection process of a 3D part.

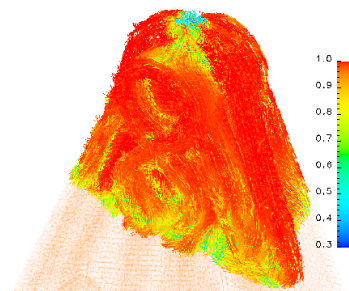


Figure 4. Fiber orientation snapshot related to the filling process illustrated in Fig. 3

SUSPENSIONS INVOLVING CNTs

When nanotubes are functionalized aggregation is prevented and the suspensions can be described by considering flow induced CNTs orientation, the same modelling approach just described. Fig. 5 illustrates nonlinear rheology as well as the fitting when assuming a standard orientation based model.

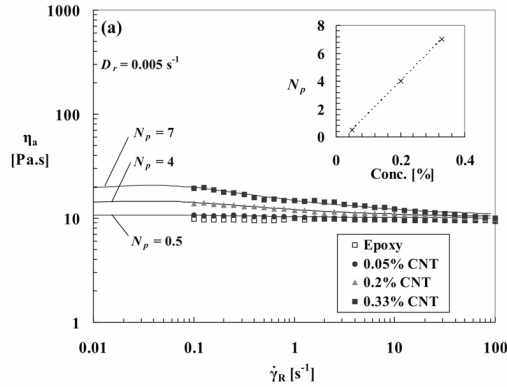


Figure 5. Nonlinear rheology of functionalized CNTs dispersed in a Newtonian matrix.

When CNTs are not functionalized the flow curves differ significantly from the ones related to functionalized CNTs as depicted in Fig. 6.

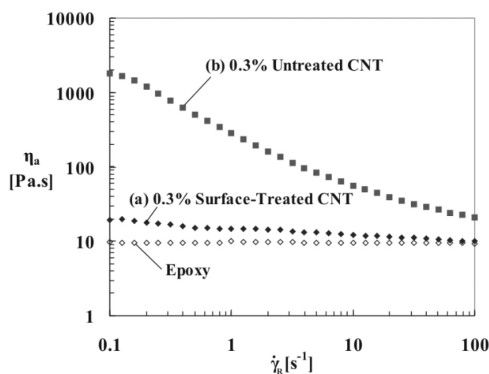


Figure 6. Apparent viscosity of functionalized versus non-functionalized CNTs suspensions

The differences in the rheological behavior were explained in¹³ in terms of flow induced aggregation / disaggregation. The proposed model involved two conformation coordinates: (i) the orientation and (ii) an extra-coordinate quantifying the aggregation state, where the two limits values describe free and fully entangled systems. The three resulting rheological parameters being (i) the rotary diffusion quantifying randomizing effects; (ii) the particle number, quantifying the tubes concentration and (iii) the aggregation / disaggregation ratio.

Despite its simplicity such a model allowed a perfect fitting as depicted in Fig. 7.

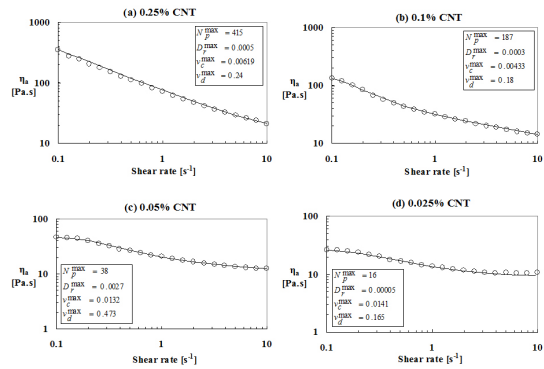


Figure 7. Modeling nonlinear rheology of non-functionalized CNTs suspensions

As just discussed the model, defined at the mesoscopic scale within the kinetic theory framework, involves the probability distribution function $\Psi(\mathbf{x}, t, n, \mathbf{p})$ giving the action of fibers that at position \mathbf{x} and time belong to a population n (describing the entanglement level: $n=0$ related to no entanglements and $n=1$ to a fully entangled system) and that are oriented in direction \mathbf{p} .

It was assumed that aggregation evolves with the shear rate because it is associated to fibers encounters whereas disaggregation

evolves with the square of the shear rate because it is associated to the energy. Thus one expects that when increasing the shear rate disaggregation dominates over aggregation and then the system should evolve towards a suspension free of entanglements. In the opposite case, when the shear rate vanishes, the systems becomes fully entangled.

Fig. 8 depicts, in the steady state regime and in an homogeneous flow where no spatial dependences are expected, i.e. $\Psi(n, \mathbf{p})$, the evolution of the marginal probability $C(n)$ defined from

$$C(n) = \oint \Psi(n, \mathbf{p}) d\mathbf{p} \quad (9)$$

As expected by increasing the flow shear-rate the density of entanglement decreases.

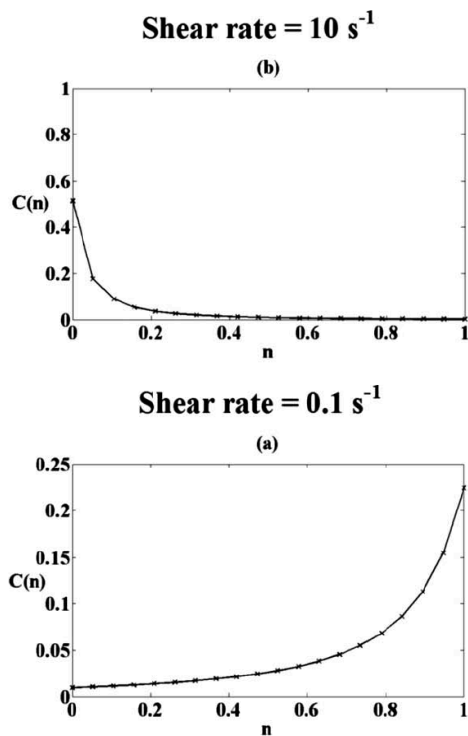


Figure 8. Evolution of the entanglements with the flow shear rate

Finally, Fig. 9 depicts the orientation state in both cases, proving that fibers tend to align in the flow direction (as expected in simple shear flows), with the alignment intensity increasing with the shear rate.

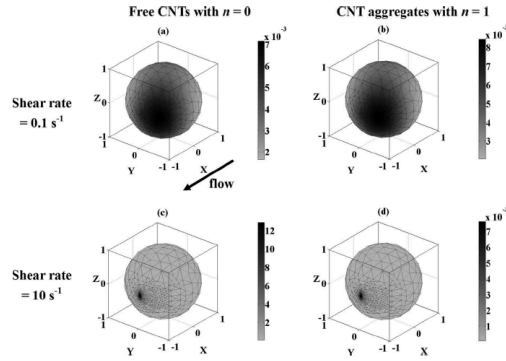


Figure 9. Orientation distribution

The resulting flow model can be then applied for simulating processes involving nanocomposites, like spin-coating. In that case a drop is placed on the surface of a rotating disc, and it spreads on its surface because the centrifugal forces. Fig. 10 depicts the device and Fig. 11 some snapshots of the fluid domain evolution and the CNTs orientation state.

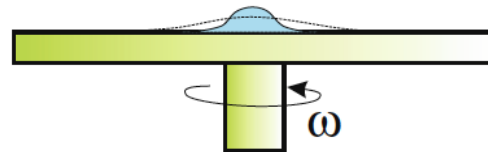


Figure 10. Sketch of spin-coating process

As soon as the orientation state is known, directional density of contacts can be evaluated and from it thermal or electrical percolation. Moreover, from this density of contacts we can derive directional resistivity that allows generating a sort of

electrical network in the functional formed part.

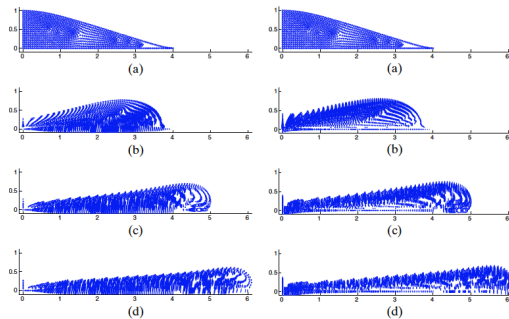


Figure 11. Evolution of the fluid domain and the CNTs orientation state during spin-coating processes

CONCLUSIONS

This work revisited the modelling and simulation of short-fibers and nano-fibers suspensions, making special emphasis in flow induced properties, in particular flow induced orientation. When considering nano-suspensions aggregation mechanism was also considered, as well as its impact on rheology and functional properties.

REFERENCES

1. Jeffery, G.B. (1922), "The motion of ellipsoidal particles immersed in a viscous fluid", *Proc. R. Soc. London*, **A102**, 161-179.
2. C. Binetruy, Chinesta, F. and Keunings, R. (2015), "Flows in polymers, reinforced polymers and composites. A multiscale approach", Springerbriefs, Springer.
3. Bird, R.B., Curtiss C.F., Armstrong, R.C. and Hassager, O. (1987), "Dynamics of polymeric liquids, Volume 2: Kinetic Theory", John Wiley and Sons.
4. Ottinger, H.C. and Laso, M. (1992), "Smart polymers in finite-element calculations", *Proc. XIth Int. Congr. on Rheology*, Elsevier, Amsterdam, 286-288.
5. Chaubal, C.V., Srinivasan, A., Egecioglu, O. and Leal, L.G. (1997), "Smoothed particle hydrodynamics techniques for the

solution of kinetic theory problems", *J. Non-Newtonian Fluid Mech.*, **70**, 125-154, 1997.

6. Lozinski, A. and Chauviere, C. (2003), "A fast solver for Fokker-Planck equation applied to viscoelastic flows calculations: 2D FENE model", *J. Computational Physics*, **189**, 607-625.

7. Ammar, A., Mokdad, B., Chinesta, F. and Keunings R. (2006), "A new family of solvers for some classes of multidimensional partial differential equations encountered in kinetic theory modeling of complex fluids", *J. Non-Newtonian Fluid Mech.*, **139**, 153-176.

8. Chinesta, F., Keunings, R. and Leygue, A. (2014), "The Proper Generalized Decomposition for advanced numerical simulations. A primer", Springerbriefs, Springer.

9. Advani, S. and Tucker, Ch. (1987), "The use of tensors to describe and predict fiber orientation in short fiber composites", *J. Rheol.*, **31**, 751-784.

10. Folgar, F. and Tucker, Ch. (1984), "Orientation behavior of fibers in concentrated suspensions", *J. Reinf. Plast. Comp.*, **3**, 98-119.

11. Petrie, C. (1999), "The rheology of fibre suspensions", *J. Non-Newtonian Fluid Mech.*, **87**, 369-402.

12. Phelps, J. and Tucker, Ch. (2009), "An anisotropic rotary diffusion model for fiber orientation in short and long fiber thermoplastics", *Journal of Non-Newtonian Fluid Mech.*, **156/3**, 165-176.

13. Ma, A., Chinesta, F., Ammar, A. and Mackley, M. (2008), "Rheological modelling of Carbon Nanotube aggregate suspensions", *Journal of Rheology*, **52/6**, 1311-1330.

14. Cruz, C., Chinesta, F. and Regnier, G. (2012), "Review on the Brownian dynamics simulation of bead-rod-spring models encountered in computational rheology", *Archives of Computational Methods in Engineering*, **19/2**, 227-259.